Supplementary Information

Extracellular vesicles from apoptotic BMSCs ameliorate osteoporosis via transporting regenerative signals

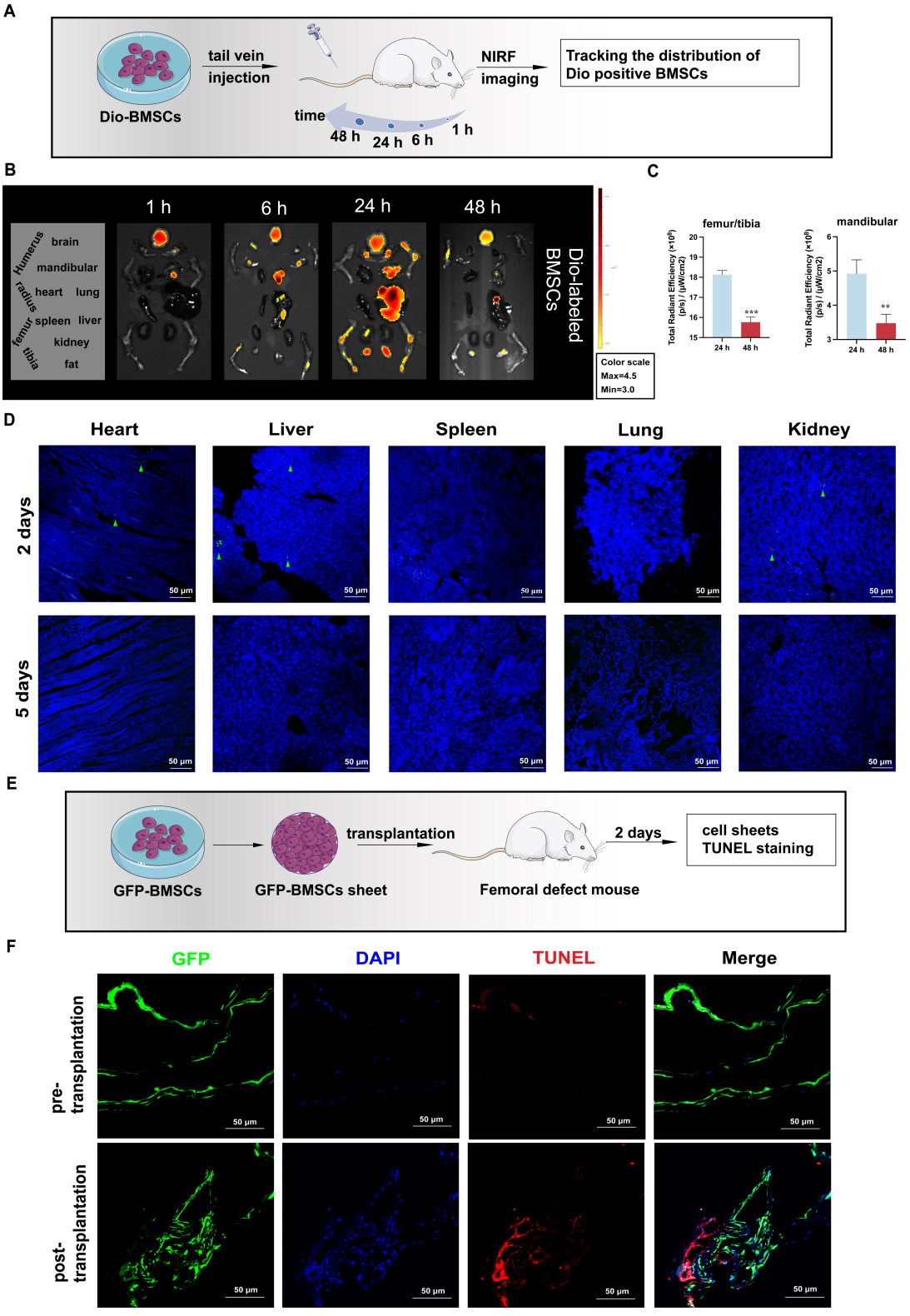

Figure S1. BMSCs undergo apoptosis post-transplantation. (**A**) Schematic diagram outlining the experimental design for tracking the fate of BMSCs post-transplantation. (**B**) Fluorescence images depicting major organs at 1 h, 6 h, 24 h, and 48 h after injection of Dio-labeled BMSCs. (**C**) Analysis Fluorescence intensity in femur/tibia and mandibula 24 h and 48 h after injection of Dio-labeled BMSCs. (**D**) Confocal assay of ZsGreen-BMSCs distribution in various organs (heart, liver, spleen, lung, kidney) after 2 and 5 days of tail vein injection of ZsGreen-BMSCs. Scale bar: 50 μm. (**E**) Schematic diagram illustrating the experimental design for detecting the apoptosis of GFP-BMSCs post-transplantation into femoral defect mice. (**F**) TUNEL staining showing GFP^+ BMSCs undergo apoptosis. Scale bar: 50 μm. Data are means ± SEMs. Statistical significance was determined by a two-tailed paired t-test in (C). **P < 0.01, ***P < 0.001.

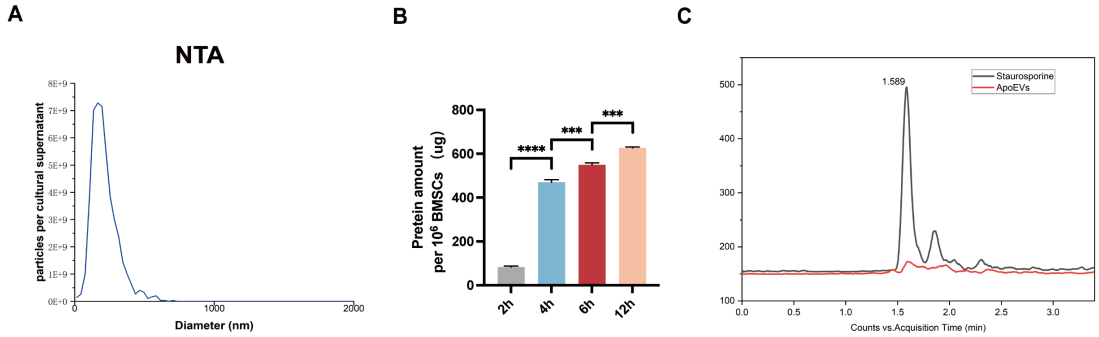

Figure S2. Identifying of ApoEVs. (A) NTA showed the diameter range and nanoparticles of ApoMVs. **(B)** BCA detects the protein amount of ApoEVs from 1×10^6 BMSCs after STS inducing apoptosis at different times. **(C)** HPLC-MS/MS showed no STS residue in the extracted ApoEVs compared to the positive control group containing only STS drugs. ***P < 0.001.

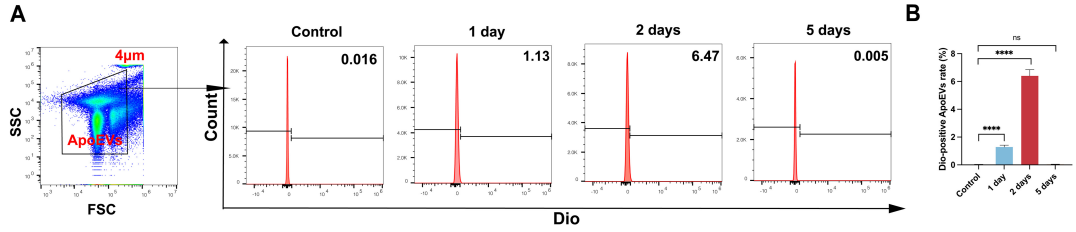

Figure S3. ApoEVs production at different times after tail vein injection of Dio-BMSCs. (A-B) The Dio-labeled ApoEVs were detected by FCM after Dio-BMSCs were injected at different times. Not significant (ns) = P > 0.05, ****P < 0.0001.

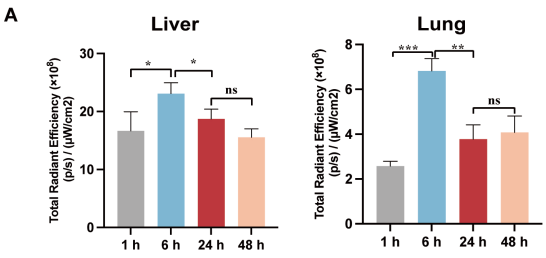

Figure S4. ApoEVs accumulate in liver and lung. (**A**) Fluorescence intensity analysis of the liver and lungs at 1 h, 6 h, 24 h, and 48 h after injection of Dio-labeled ApoEVs. Data are means ± SEMs. Statistical significance was determined by a two-tailed paired t-test in (A). Not significant (ns) = P > 0.05, *P < 0.05, **P < 0.01, ***P < 0.001.

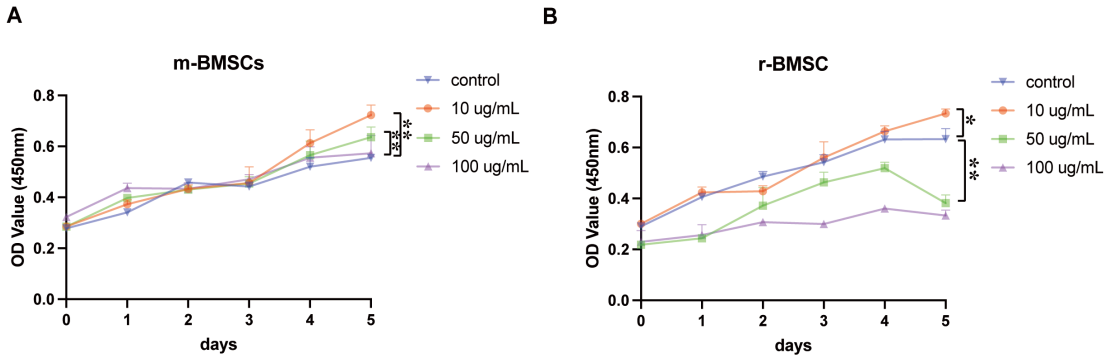

Figure S5. ApoEVs promoted the proliferation of BMSCs in low concentrations. (A) The effect of 10 μg/mL 50μg/mL and 100 μg/mL ApoEVs on the proliferation ability of m-BMCSs. **(B)** The effect of 10 μg/mL, 50 μg/mL, and 100 μg/mL ApoEVs on the proliferation ability of r-BMCSs. *P < 0.05, **P < 0.01.

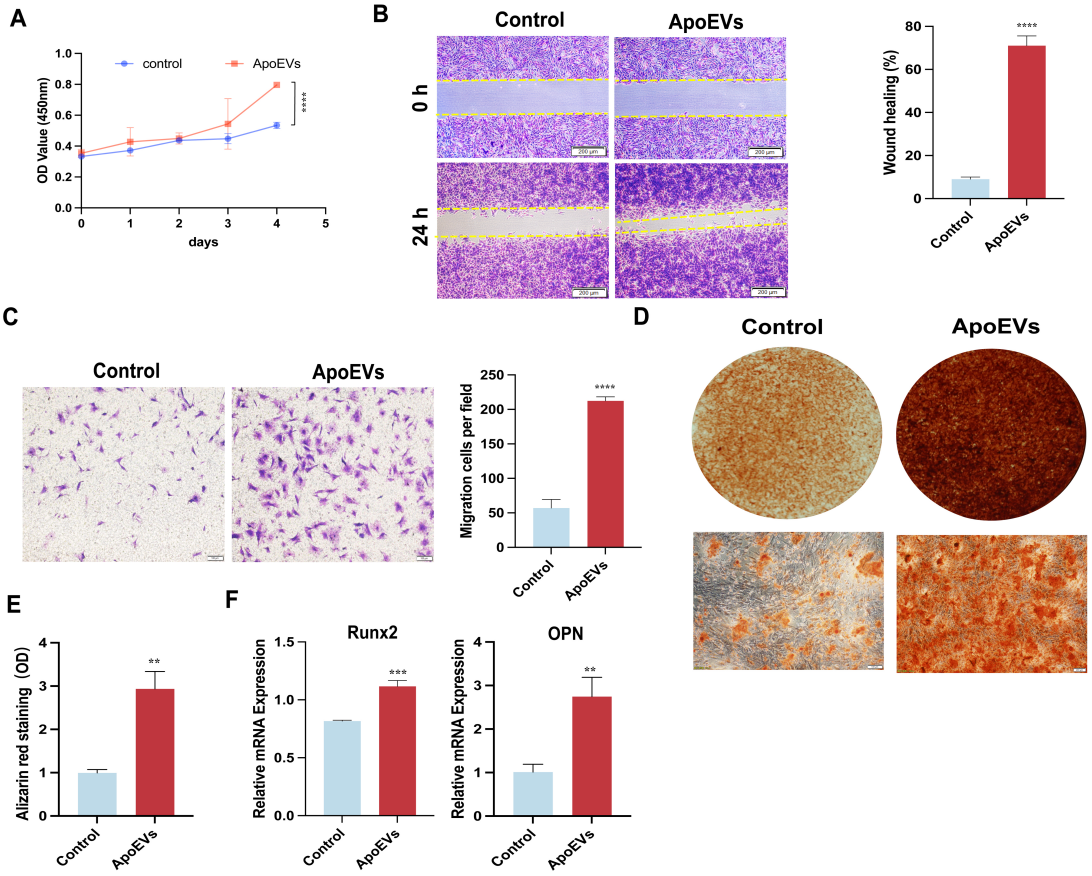

Figure S6. The effect of ApoEVs on the proliferation, migration, and osteogenic differentiation of r-BMSCs. (**A**) The effect of ApoEVs on the proliferation ability of BMSCs was measured by the CCK-8 assay. (**B**) Scratch healing assay and transwell assay (**C**) illustrate the effect of ApoEVs on the migration and invasion ability of BMSCs. Scale bar: 200 μm (B), and 100 μm (C). (**D-E**) ApoEVs increased the mineralized nodule formation of BMSCs during osteogenic induction, as assessed by alizarin red staining. Scale bar: 100 μm (**F**) ApoEVs from r-BMSCs promote the expression of Runx2 and OPN, as assessed by qRT-PCR. Data are means ± SEMs. Statistical significance was determined by a two-tailed paired t-test in (A, B, C, E, F). Not significant (ns) = P > 0.05, *P < 0.05, **P < 0.01, ***P < 0.001, ****P < 0.0001.

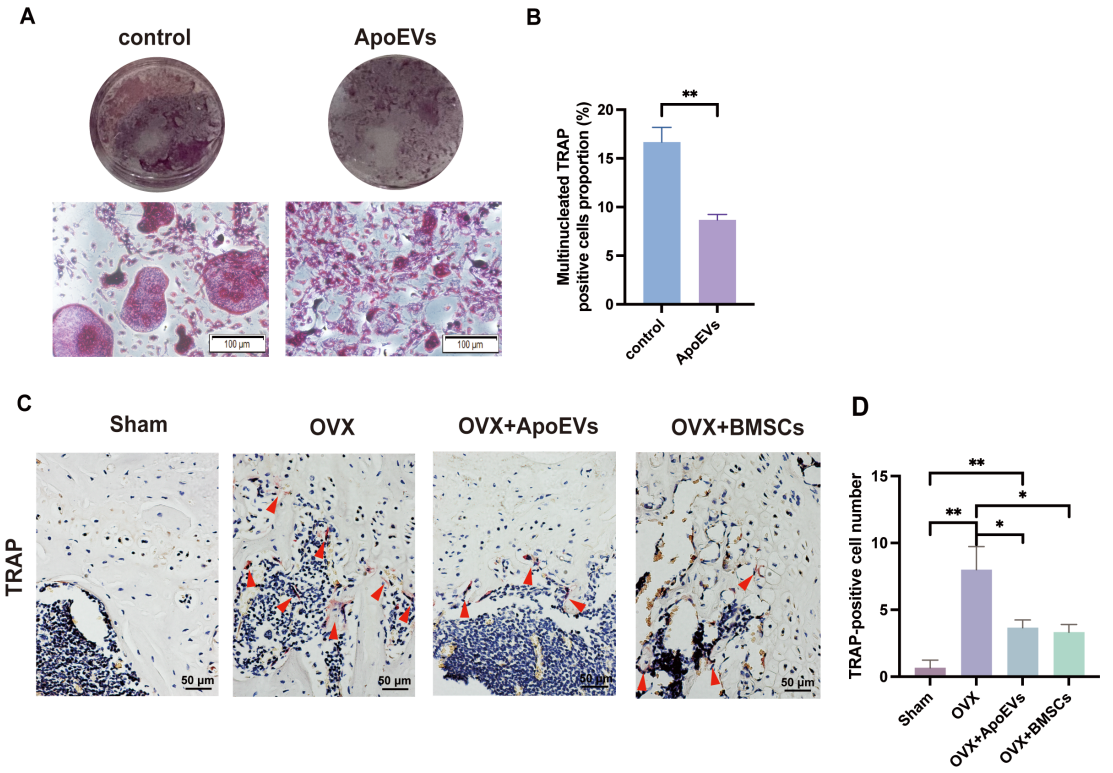

Figure S7. The effect of ApoEVs on osteoclasts. (A-B) Trap stain showed that ApoEVs inhibit osteoclast formation. Scale bar: 100 μm. **(C-D)** ApoEVs inhibit bone resorption as assessed by Trap-stained femur slices. Scale bar: 50 μm. *P < 0.05, **P < 0.01.

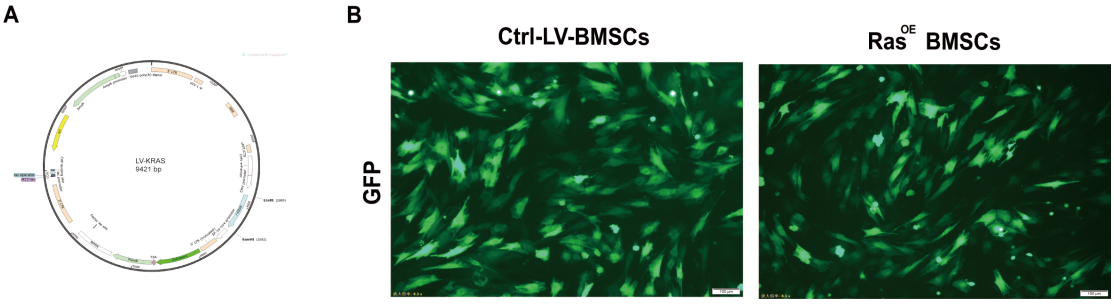

Figure S8. Ras lentivirus successfully transfected into BMSCs. (**A**) Schematic diagram outlining the gene targeting strategy for generating Ras overexpression in lentivirus. (**B**) GFP-Ras lentivirus successfully transfected into BMSCs. Scale bar: 100 μm.

Table S1. The sequences of the qRT-PCR primers.

Gene	Forward primer sequence 5′→3'	Reverse primer sequence 5′→3'
Mouse		
ALP	TTGTGCCAGAGAAAGAGA	GTTTCAGGGCATTTTTCAAGGT
RUNX2	CCGCACGACAACCGCACCAT	CGCTCCGGCCCACAATCTC
OCN	CTGACAAAGCCTTCATGTCCAA	GCGCCGGAGTCTGTTCACTA

Ras	GCTCACCATCCAGTTCATCCAGTC	GGCTGCTCTGTCATCTATCACACAC
Raf1	CAGATGTGGCACGGAGCAACC	CTCGGACTGTAACTCCACACCTTG
MEK	TCATCTGGAGATCAAACCCGCAATC	CCATCGCTGTAGAACGCACCATAG
ERK1/2	CCACCTGTGAAGAATGAACT	CACCTTTCTCTGTCTTTATCGT
Ki67	CACAGAGAACAAAGGTGTGAAG	GGAGACTGCAGAGCTATTTTTG
cyclinD2	TGGGAAGTTTTGTTGGGTCA	TCCTTGTCCAGGTAATGCCA
CDK2	CCTGCTTATCAATGCAGAGGG	GTGCTGGGTACACACTAGGTG
Gapdh	AAGAAGGTGGTGAAGCAGGCATC	CGGCATCGAAGGTGGAAGAGTG
Rat		
RUNX2	TCATTTGCAsCTGGGTCACAT	TCTCAGCCATGTTTGTGCTC
OPN	AAGCGTGGAAACACACAGC	CTTTGGAACTCGCCTGACTG
Gapdh	TATGACTCTACCCACGGCAAG	TACTCAGCACCAGCATCACC

Table S2. The sequences of the siRNA primers.

Gene	**Forward primer sequence 5′→3'**	**Reverse primer sequence 5′→3'**
siRNA NC	UUCUCCGAACGUGUCACGUTT	ACGUGACACGUUCGGAGAATT
siRNA PC	CCCUCACAAGAGGAUUGAATT	UUCAAUCCUCUUGUGAGGGTT
siKRAS	CCAUUAUAGAGAACAAAUUTT	AAUUUGUUCUCUAUAAUGGTT